

WSF-CT-11, a Sesquiterpene Derivative, Activates AMP-Activated Protein Kinase with Anti-diabetic Effects in 3T3-L1 Adipocytes

Yang Yang, Yunyun Wang, Zhijie Zhang, Shifa Wang,* and Zhen Li*

Cite This: *ACS Omega* 2021, 6, 31272–31281

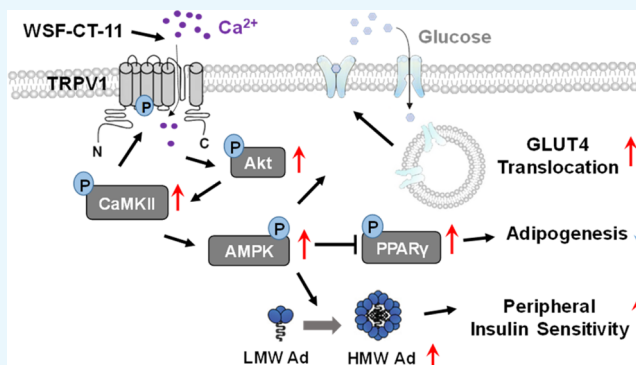
Read Online

ACCESS |

Metrics & More

Article Recommendations

ABSTRACT: Background: AMP-activated protein kinase (AMPK) is a therapeutic target against type II diabetes (T2D). Synthetic sesquiterpene derivatives were investigated to identify novel AMPK activators as anti-diabetic drugs because the leading drugs like metformin and thiazolidinediones (TZDs) activate AMPK by inhibiting the synthesis of adenosine 5'-triphosphate and thus are associated with some side effects. Results: We identified WSF-CT-11 as an AMPK activator in HEK293T cells and found that WSF-CT-11 activates AMPK by the activation of transient receptor potential vanilloid type 1 (TRPV1), a Ca^{2+} -permeable cation channel. The increased Ca^{2+} influx then activates phosphoinositide 3-kinase (PI3K), protein kinase B (PKB/Akt), and Ca^{2+} /calmodulin-dependent protein kinase II (CaMKII), which in turn phosphorylates TRPV1 and facilitates the formation of a TRPV1/Akt/CaMKII/AMPK complex. This complex might be important for the regulation of AMPK activity. In 3T3-L1 adipocytes, WSF-CT-11-induced AMPK activation has three anti-diabetic effects. It promotes the assembly of high-molecular-weight adiponectin, which has stronger insulin-sensitizing activity than other multimers. It improves translocation of the glucose transporter type 4, increases glucose uptake, and induces the inhibitory phosphorylation of peroxisome proliferator-activated receptor γ and thus suppresses adipogenesis. Conclusion: WSF-CT-11 is a novel AMPK activator and potential drug against T2D without the side effects of metformin and TZDs.



1. INTRODUCTION

T2D is a silent epidemic three times as deadly as the coronavirus disease of 2019, and its prevalence continues to rise.¹ As the need for more effective treatment continues to increase, it is urgent to develop new medications to combat T2D and its comorbidities, such as obesity and cardiovascular diseases.² Metformin (Met) and thiazolidinediones (TZDs) are among the insulin-sensitizing agents developed recently. Their anti-diabetic effects have been attributed, at least partly, to the activation of AMP-activated protein kinase (AMPK).³

AMPK, a heterotrimer with one catalytic (α) and two regulatory (β and γ) subunits, is a cellular energy sensor.⁴ The falling energy status, signified by the increased AMP/adenosine 5'-triphosphate (ATP) ratio, leads to AMPK phosphorylation, thereby inhibiting energy-consuming anabolism (such as hepatic gluconeogenesis and pancreatic insulin secretion) and promoting ATP-producing catabolism (e.g., glucose uptake and glycolysis in muscle and adipose tissues).⁵ Met and TZDs activate AMPK by inhibiting complex I of the respiratory chain, disrupting the ATP synthesis, and increasing the AMP/ATP ratio and thus are associated with some side effects, such as lactic acidosis and diarrhea.⁶ The promotion of Ca^{2+} influx also activates AMPK. For example, evodiamine (Evo) activates AMPK by the Ca^{2+} -dependent PI3K/Akt/CaMKII signaling,⁷

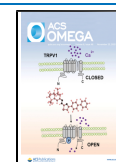
while A23187 and osmotic stress activate AMPK by Ca^{2+} /calmodulin-dependent protein kinase kinase β (CaMKK β). A769662 activates AMPK by directly binding to the β subunit.⁶ However, it is unlikely to be used therapeutically because of the poor oral absorption and off-target effects.⁴ Therefore, it is urgent to identify novel AMPK activators for anti-diabetic treatment.

White adipose tissue is an active endocrine organ that not only stores energy but also participates in the maintenance of metabolic homeostasis.⁸ It plays a major role in the regulation of whole-body insulin sensitivity. First, it secretes a number of serum adipokines, among which adiponectin (Ad) is the most abundant.⁹ The major function of Ad is to enhance insulin sensitivity. The reduced plasma concentration of Ad is correlated with T2D and its comorbidities.¹⁰ Ad is assembled into different multimers in adipocytes, the low-molecular-

Received: September 13, 2021

Accepted: October 18, 2021

Published: October 28, 2021



weight (LMW) form or trimer, the middle-molecular-weight (MMW) form or hexamer, and the high-molecular-weight (HMW) form composed of 18–36 oligomers.^{11,12} HMW Ad possesses the strongest insulin-sensitizing activity with the ratio of HMW to total Ad being a potent predictor of hepatic insulin sensitivity. Its assembly is tightly regulated by adipocytes because these multimers do not interconvert after secretion.¹³ Second, a major response of insulin stimulation is to promote glucose uptake in the muscle and adipose tissues. The principal glucose transporter that mediates this process is glucose transporter type 4 (GLUT4).¹⁴ The translocation of GLUT4 from the cytoplasm to the cell membrane is reported to be critical for the restoration of postprandial glucose and is defective in T2D.¹⁵ Third, obesity is involved in the pathogenesis of T2D and its complications,² which suggests that increased adipogenesis could induce insulin resistance. Indeed, the inhibition of proliferator-activated receptor γ (PPAR γ), a master regulator of adipogenesis, is downstream of AMPK activation and thus is associated with the increase of insulin sensitivity.¹⁶ In other words, agents with these anti-diabetic effects in adipocytes could be potential drugs against T2D and its comorbidities.

In the present study, we searched among 11 sesquiterpene derivatives (WSF-CT-1 to WSF-CT-11) and identified two molecules, WSF-CT-10 and WSF-CT-11 (Figure 1), as novel

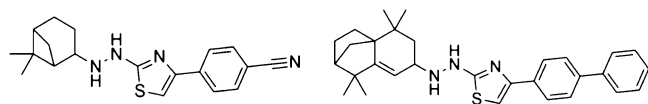


Figure 1. Structure of WSF-CT-10 and WSF-CT-11. Structural formula of 2-(2-(6,6-dimethylbicyclo[3,1,1]hept-2-yl)hydrazino)-4-(4-cyanophenyl)thiazole (WSF-CT-10, left) and 4-([1,1'-biphenyl]-4-yl)-2-(2-(1,1,5,5-tetramethyl-1,2,3,4,5,6-hexahydro-7H-2,4a-methanonaphthalen-7-yl)hydrazineyl)thiazole (WSF-CT-11, right).

AMPK activators. WSF-CT-10 was excluded for further research due to its inhibition of ATP synthesis. We found that WSF-CT-11 activates AMPK by the Ca²⁺-dependent PI3K/Akt/CaMKII pathway, and this activation could promote the assembly of HMW Ad, improve GLUT4 translocation, and inhibit adipogenesis in 3T3-L1 adipocytes.

2. RESULTS

2.1. WSF-CT-10 Activates AMPK by Inhibiting ATP Synthesis and WSF-CT-11 Activates AMPK by Promoting Ca²⁺ Influx. To identify novel AMPK activators as antidiabetic drugs, HEK293T cells were treated with 11 sesquiterpene derivatives for 1 h. WSF-CT-10 and WSF-CT-11 significantly increased the phosphorylation of AMPK and thus are AMPK activators (Figure 2A). To support this discovery, we used compound C (CC), a specific AMPK antagonist, to pretreat cells and found that WSF-CT-10- and WSF-CT-11-induced AMPK activation was abrogated (Figure 2B).

We then investigated the mechanisms in which WSF-CT-10 and WSF-CT-11 activate AMPK. High-performance liquid chromatography and flow cytometry were used to measure the levels of intracellular adenosine phosphates and Ca²⁺, respectively. The results revealed that WSF-CT-10 activates AMPK by increasing the AMP/ATP ratio (Figure 2C), while WSF-CT-11 activates AMPK by promoting Ca²⁺ influx (Figure 2D, left panel). As the inhibition of ATP synthesis was undesirable, we focused on the development of WSF-CT-11.

Pretreatment with ethylene glycol tetraacetic acid (EGTA), a calcium chelator nonpermeant to the cell membrane, abolished WSF-CT-11-induced AMPK activation (Figure 2D, right panel), which proved that WSF-CT-11 activates AMPK by the calcium-mediated pathway.

2.2. WSF-CT-11 Activates AMPK by TRPV1 and Ca²⁺-Dependent PI3K/Akt/CaMKII Signaling. To identify the CaMK upstream of WSF-CT-11-induced AMPK activation, HEK293T cells were pretreated with STO-609 or KN62, selective inhibitors of CaMKK β and CaMKII, respectively. The results indicated that KN62 abolished WSF-CT-11-elicited AMPK activation (Figure 3A), which suggests that CaMKII is the upstream CaMK that activates AMPK by WSF-CT-11 treatment.

Evo activates AMPK by TRPV1 and the Ca²⁺-dependent PI3K/Akt/CaMKII pathway and thus is a potential drug against T2D and its comorbidities.⁷ Pretreatment with inhibitors of this pathway, such as capsazepine (CPZ, a TRPV1 antagonist), LY294002 (LY, a PI3K inhibitor), and KN62 (a CaMKII inhibitor) abrogated WSF-CT-11-induced AMPK activation (Figure 3B), which suggests that TRPV1 and PI3K/Akt/CaMKII pathway are upstream of WSF-CT-11-induced AMPK activation. To demonstrate this discovery, we detected the levels of phosphorylated Akt and CaMKII and found that TRPV1 and PI3K are upstream of Akt and CaMKII, and Akt is upstream of CaMKII (Figure 3C). By measuring the levels of intracellular Ca²⁺, we proved that the calcium influx is induced by TRPV1 activation (Figure 3D).

The activated PI3K/Akt/CaMKII signaling could phosphorylate TRPV1 and promote the formation of a TRPV1/Akt/CaMKII complex, which might be important for the improvement of endothelial function.¹⁷ We then investigated whether this process is also implicated in WSF-CT-11-induced AMPK activation. Immunoprecipitation (IP) assay revealed that WSF-CT-11 promoted the phosphorylation of TRPV1; the inhibition of PI3K and CaMKII abolished this effect, while the inhibition of AMPK could not (Figure 4A). This suggests that PI3K/Akt/CaMKII signaling is upstream of WSF-CT-11-induced TRPV1 phosphorylation. To determine whether the phosphorylated TRPV1 could recruit the complex responsible for AMPK activation, we used IP assay to find that, like Evo, WSF-CT-11 could promote the interaction of TRPV1 with Akt, CaMKII, and AMPK, and the activation of PI3K/Akt/CaMKII signaling is upstream of this effect (Figure 4B). The formation of this TRPV1/Akt/CaMKII complex might be upstream of and important for the activation of AMPK (Figure 4C).

2.3. WSF-CT-11-Induced AMPK Activation Could Promote the Assembly of HMW Ad in 3T3-L1 Adipocytes. We have demonstrated that Evo-induced AMPK activation could promote the assembly of HMW Ad.¹⁸ To find out whether WSF-CT-11 treatment has a similar effect, we first proved that WSF-CT-11 could activate AMPK in 3T3-L1 adipocytes (Figure 5A), then treated cells for 48 h, and detected the levels of Ad multimers by native-polyacrylamide gel electrophoresis (PAGE) and western blot. The results revealed that WSF-CT-11 could inhibit the expression of total Ad, reduce the levels of LMW and MMW Ad, and promote the assembly of HMW Ad, leading to a significant increase in the ratio of HMW/total Ad (Figure 5B). This effect was abolished after AMPK knockdown (Figure 5B), which indicates that WSF-CT-11-induced AMPK activation is upstream of the increased assembly of HMW Ad.

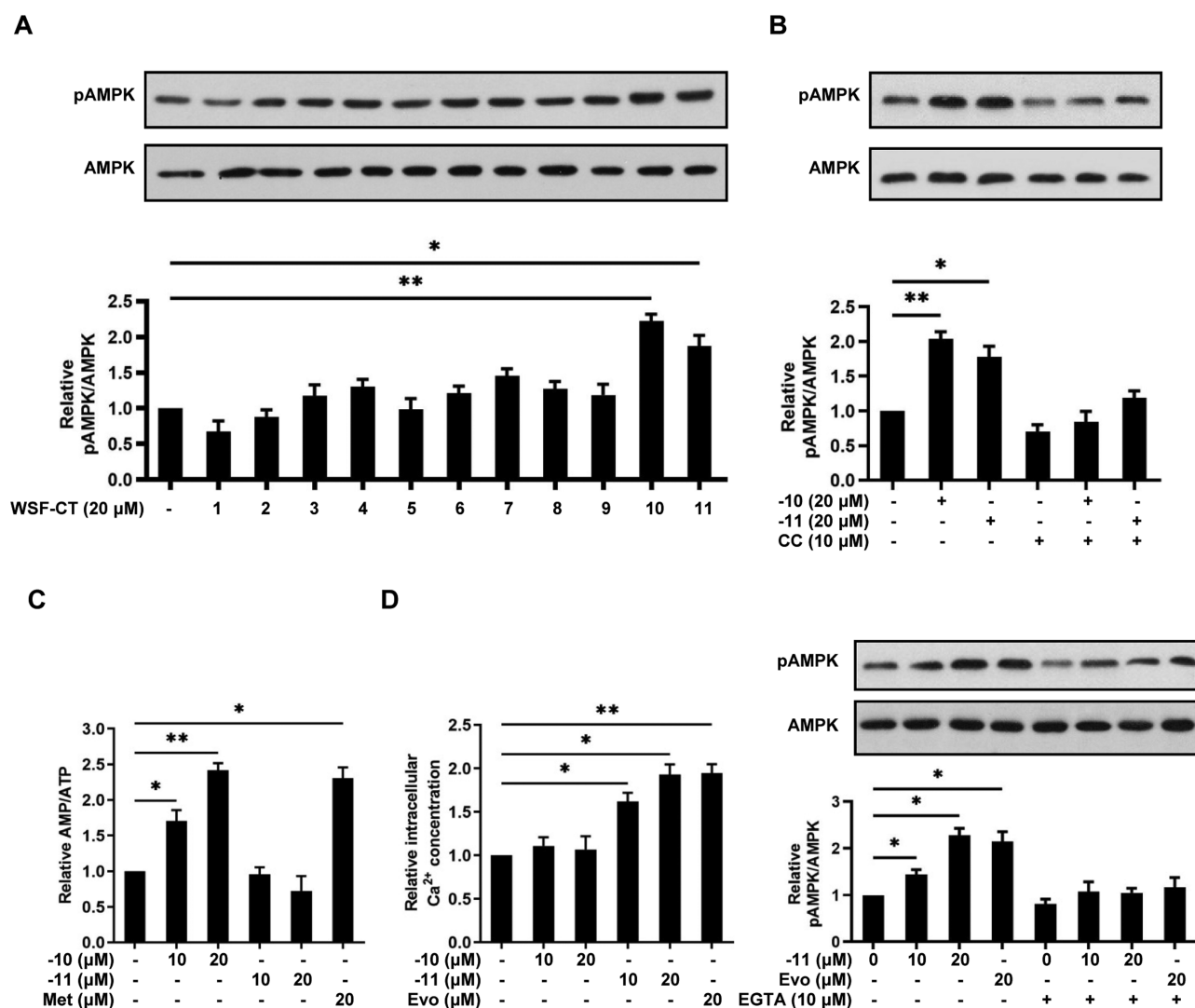


Figure 2. WSF-CT-10 activates AMPK by inhibiting ATP synthesis, while WSF-CT-11 activates AMPK by promoting Ca^{2+} influx. (A) HEK293T cells were treated with 11 synthetic sesquiterpene derivatives (WSF-CT-1 to WSF-CT-11) for 1 h and then immunoblotted for the levels of phosphorylated AMPK α (Thr172) and AMPK α . (B) Cells were treated with CC for 1 h and WSF-CT-10 (-10) or WSF-CT-11 (-11) for another hour. (C) Cells were treated with -10, -11 or Met for 1 h. Intracellular levels of adenosine phosphates were determined by high-performance liquid chromatography. (D, left panel) Cells were treated with -10, -11 or Evo for 1 h. Intracellular Ca^{2+} levels were analyzed by flow cytometry. (D, right panel) Cells were treated with EGTA for 1 h and -11 or Evo for another hour. $n = 3$; * $p < 0.05$, ** $p < 0.01$ vs vehicle-treated group.

2.4. WSF-CT-11-Induced AMPK Activation Could Increase Glucose Uptake and Inhibit Adipogenesis in 3T3-L1 Adipocytes.

Met promotes glucose uptake by AMPK activation and the subsequent increase in GLUT4 translocation in 3T3-L1 preadipocytes.³ To explore whether WSF-CT-11 could exert similar effects in mature adipocytes, the cells were treated with WSF-CT-11 for 1 h and lysed to isolate membrane proteins. The level of GLUT4 increased in the membrane and decreased in the cytoplasm in dose-dependent manners (Figure 6A), which indicates that WSF-CT-11 could promote the translocation of GLUT4 from the cytoplasmic storage sites to the cell membrane. To illustrate the effect of WSF-CT-11-elicited GLUT4 translocation, we performed glucose uptake assay and found that WSF-CT-11 increased the intracellular uptake of 2-deoxyglucose, a glucose analogue (Figure 6B). The pretreatment of CC reduced this effect (Figure 6B), which proves that AMPK activation is important for WSF-CT-11-induced glucose uptake. In conclusion, WSF-

CT-11 could increase glucose uptake by activating AMPK and promoting GLUT4 translocation in 3T3-L1 adipocytes.

With a PPAR γ responsive element in the promoter,¹⁹ Ad expression is possibly downregulated by the inhibition of PPAR γ .^{20,21} It was reported that berberine (BBR) could protect against obesity by the activation of AMPK and the inhibitory phosphorylation of PPAR γ .^{16,22} To explore whether WSF-CT-11 could inhibit adipogenesis in 3T3-L1 preadipocytes, we induced cells to differentiate in the presence of WSF-CT-11 and used oil red staining to assess their degree of differentiation. The size and amount of the lipid droplet decreased in dose-dependent manners (Figure 6C), which indicates that WSF-CT-11 could inhibit adipogenesis. To demonstrate that WSF-CT-11 inhibits adipogenesis by the inhibitory phosphorylation of PPAR γ , we treated 3T3-L1 adipocytes for 1 h and found that the level of phosphorylated PPAR γ showed a dose-dependent increase, and this effect was downstream of AMPK activation (Figure 6D).

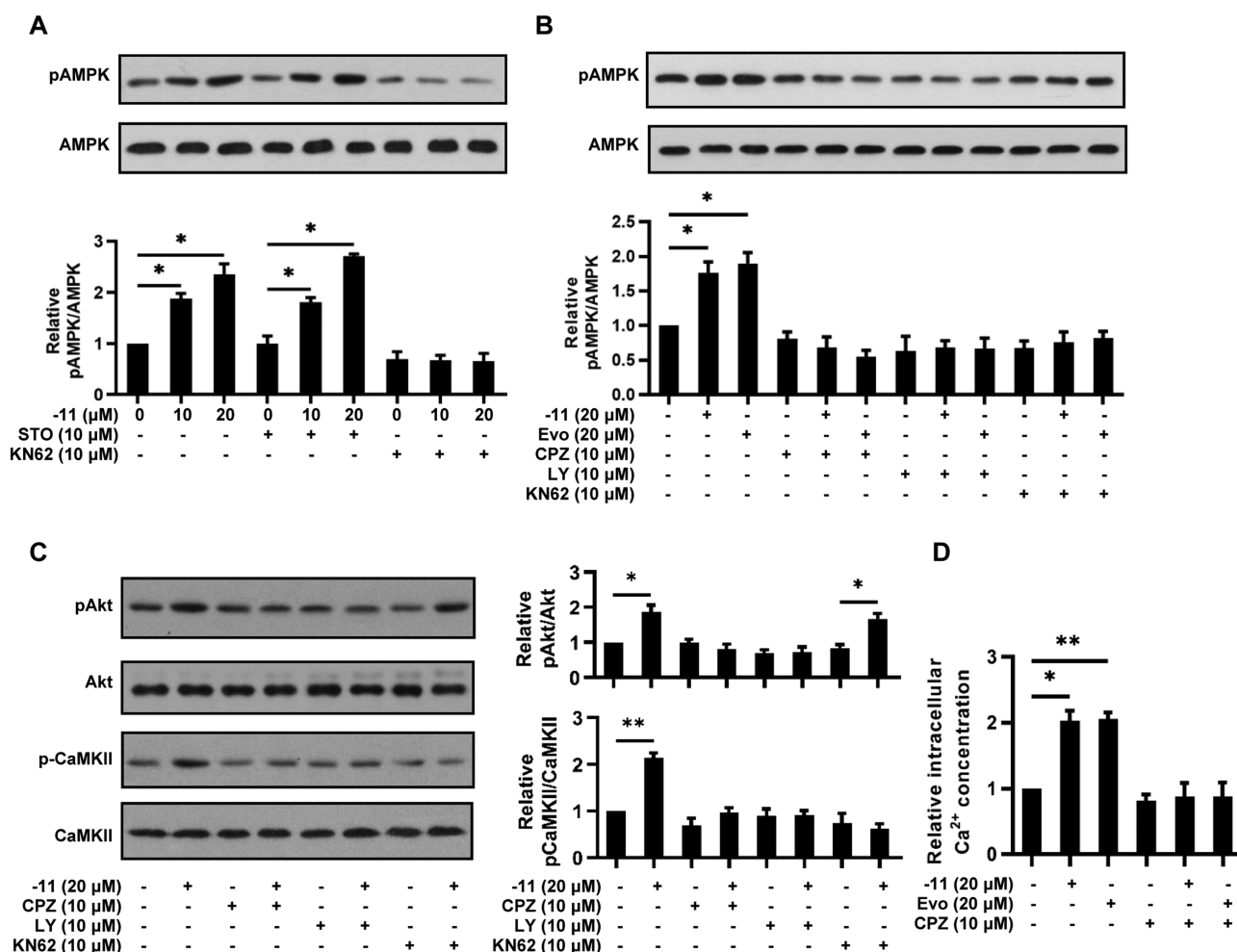


Figure 3. WSF-CT-11 activates AMPK by TRPV1 and Ca²⁺-dependent PI3K/Akt/CaMKII signaling. (A) HEK293T cells were treated with STO-609 (STO) or KN62 for 1 h and WSF-CT-11 (−11) for another hour. (B,C) Cells were treated with CPZ, LY, or KN62 for 1 h and −11 for another hour and then immunoblotted for the levels of phosphorylated AMPKα (Thr172), AMPKα (B), phosphorylated Akt (Ser473), Akt, phosphorylated CaMKII (Thr286), and CaMKII (C). (D) Cells were treated with CPZ for 1 h and −11 for another hour. Intracellular Ca²⁺ levels were then measured by flow cytometry. *n* = 3; **p* < 0.05, ***p* < 0.01 vs vehicle-treated group.

Evidence suggests that PPAR γ could induce the expression of a CCAAT/enhancer binding protein (C/EBP α), which in turn promotes PPAR γ transcription. As master regulators of adipogenesis, PPAR γ and C/EBP α act synergistically to upregulate lipid-metabolizing proteins, including the adipocyte fatty acid-binding protein (aP2).²⁰ To explore whether WSF-CT-11-induced PPAR γ phosphorylation could inhibit the transcription of these responsive genes, 3T3-L1 preadipocytes were treated during differentiation and subjected to quantitative real-time polymerase chain reaction (qRT-PCR). Results indicated that WSF-CT-11 inhibited the transcription of PPAR γ , C/EBP α , and aP2, and AMPK activation was upstream of these effects (Figure 6E). In conclusion, WSF-CT-11-induced AMPK activation could suppress adipogenesis by the phosphorylation of PPAR γ and the inhibition of its responsive genes like PPAR γ , C/EBP α , and aP2.

3. CONCLUSIONS

In this study, we targeted AMPK to identify novel drugs against T2D and found that WSF-CT-11, a sesquiterpene derivative, could integrate the channel (the stimulation of Ca²⁺ influx and PI3K/Akt/CaMKII signaling) and scaffold (the recruitment of Akt, CaMKII, and AMPK) functions of TRPV1

to activate AMPK. This activation could exert three anti-diabetic effects in 3T3-L1 adipocytes: (1) increasing GLUT4 translocation and glucose uptake, (2) inhibiting PPAR γ activity and adipogenesis, and (3) promoting the assembly of HMW Ad, which increases peripheral insulin sensitivity (Figure 7). However, some issues still remain to be elucidated.

3.1. TRPV1 is a Potential Target against T2D. TRPV1 is sensitive to pungent compounds (such as capsaicin) and noxious stimuli (such as protons, heat, low pH, and inflammatory factors).²³ It is mainly expressed in nociceptors and is demonstrated to be an important target for the treatment of chronic pain like cancer and musculoskeletal pain.²⁴ Evidence suggests that TRPV1 is an important sensor and regulator in nonneuronal cells as well, and its ligands could protect against T2D comorbidities such as cardiovascular diseases.²⁵ For example, capsaicin could reduce blood pressure and delay the onset of stroke in hypertensive rats by the phosphorylation of protein kinase A (PKA) and endothelium-dependent vasodilation.²⁵

In HEK293T cells, TRPV1 could function not only as an ion channel but also as a scaffold. The phosphorylation of TRPV1 by PI3K/Akt/CaMKII signaling might promote its channel activity and facilitate protein–protein interactions to activate

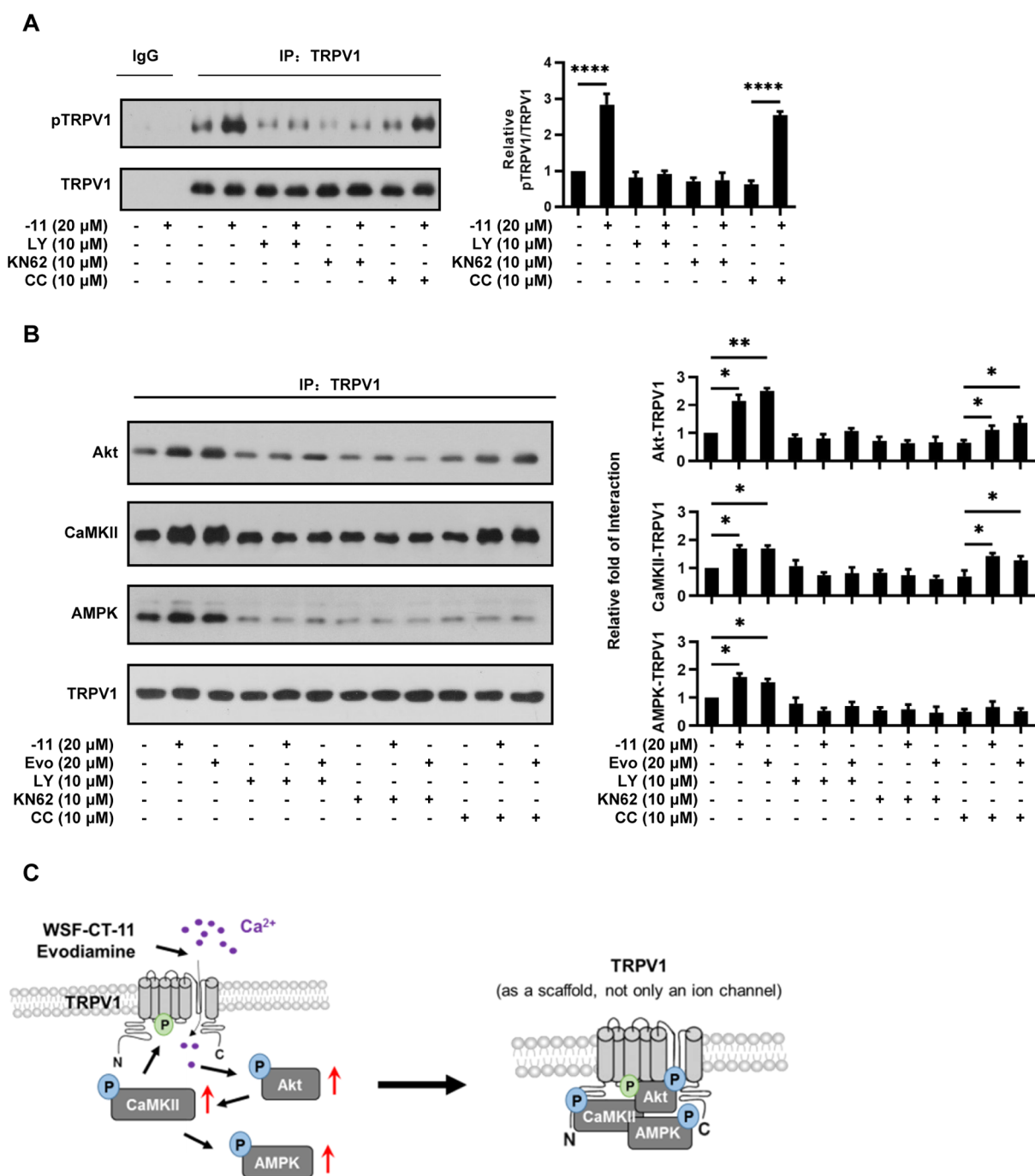


Figure 4. WSF-CT-11 promotes the phosphorylation of TRPV1 and the formation of a TRPV1/Akt/CaMKII/AMPK complex. (A,B) HEK293T cells were treated with CPZ, LY, or KN62 for 1 h and -11 or Evo for another hour. Cell lysates were immunoprecipitated with nontargeting IgG or anti-TRPV1 antibody. The levels of phosphorylated TRPV1 (A), Akt, CaMKII, AMPK (B), and TRPV1 in the precipitates were determined by western blot. (C) Schematic diagram of the mechanism by which -11 activates AMPK. -11 activates TRPV1 and the Ca^{2+} -dependent PI3K/Akt/CaMKII signaling, which in turn promotes the phosphorylation of TRPV1. The phosphorylated TRPV1 then functions as a scaffold for the formation of a TRPV1/Akt/CaMKII/AMPK complex, which might be important for the regulation of AMPK activity. $n = 3$; $*p < 0.05$, $**p < 0.01$, $***p < 0.0001$ vs vehicle-treated group.

AMPK. In neurons, intracellular proteins (such as PKA and CaMKII) could interact with and phosphorylate TRPV1 to further promote its channel function.²⁶ Consistent with our *in vitro* discoveries, the activation of TRPV1 by Evo in endothelial cells could also activate the Ca^{2+} -dependent PI3K/Akt/CaMKII signaling and promote TRPV1 phosphorylation and recruitment of endothelial nitric oxide (NO) synthase (eNOS). The formation of TRPV1-eNOS complex

might be important for the phosphorylation of eNOS and NO-dependent angiogenesis, which was critical for combating atherosclerosis.¹⁷

The physiological function of WSF-CT-11-induced TRPV1 and AMPK activation remains to be found. We are exploring whether WSF-CT-11 treatment could exert anti-diabetic effects, such as reduced lipogenesis and improved insulin action, in experimental animals, and constructing gene

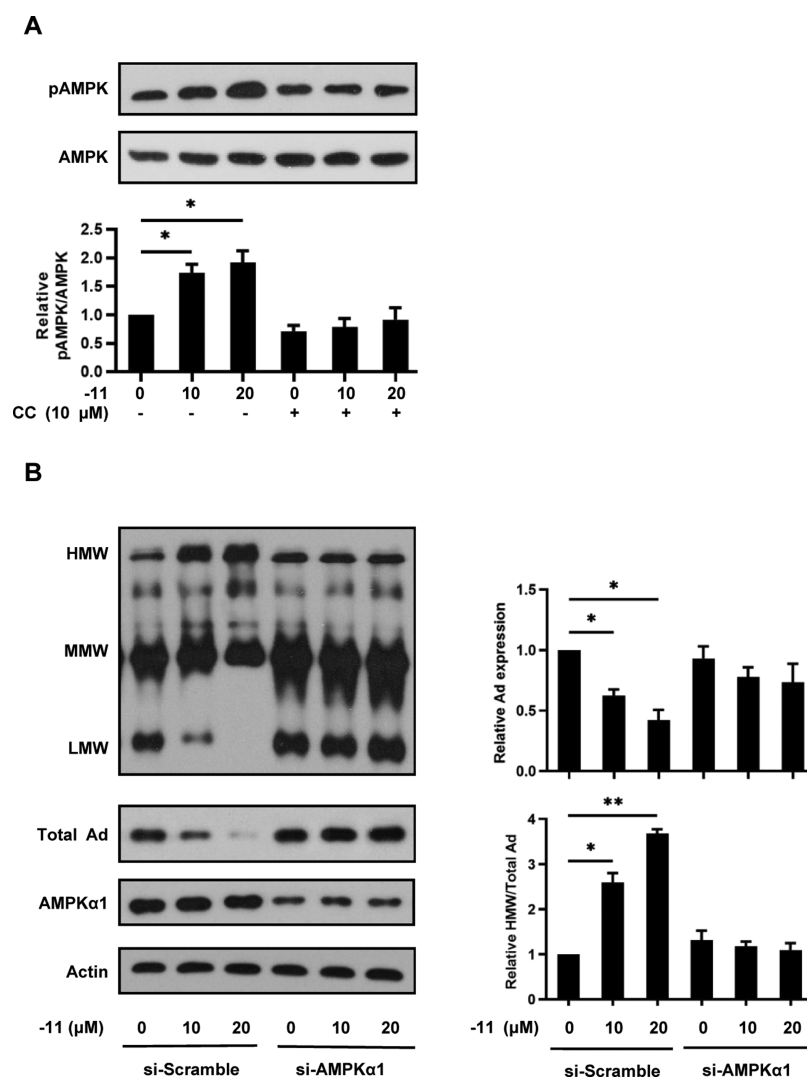


Figure 5. WSF-CT-11-induced AMPK activation could promote the assembly of HMW Ad in 3T3-L1 adipocytes. (A) 3T3-L1 adipocytes were treated with CC for 1 h and WSF-CT-11 (−11) for another hour and then immunoblotted for the levels of phosphorylated AMPK α (Thr172) and AMPK α . (B) 3T3-L1 adipocytes were transfected with scramble or AMPK α 1 siRNA for 24 h and then treated with −11 for another 24 h. Cell lysates were subjected to native-PAGE and western blot to detect the levels of LMW, MMW, and HMW Ad. The levels of total Ad, AMPK α 1, and β -actin were detected by SDS-PAGE and western blot. $n = 3$; $*p < 0.05$, $**p < 0.01$ vs vehicle-treated group.

knockout mice to investigate the function of adipose TRPV1 in these effects.

3.2. Akt and AMPK Might Act Synergistically on GLUT4 Translocation. GLUT4 plays an important part in the regulation of glucose homeostasis. Fat and muscle are the major depots for insulin-regulated glucose uptake, and GLUT4 is the main glucose transporter in these tissues.¹⁴ It is generally retained in the cytoplasm and cycles in the endosomal system. Upon insulin stimulation, the activated insulin receptor substrate (IRS) and its downstream PI3K/Akt signaling could phosphorylate TBC1D4 (AS160, a Rab GTPase-activating protein), inhibit its GTPase activity, and thus promote the translocation of GLUT4 from the cytoplasm to the cell membrane.^{27,28} This response plays a major role in the restoration of blood glucose after eating and is defective in the pathological conditions of insulin resistance.¹⁵

TBC1D1, another Rab GTPase-activating protein with TBC1 domain, also regulates GLUT4 translocation in adipocytes. It could be phosphorylated by Akt and AMPK, but AMPK is more potent in its regulation.²⁹ We observed that

the inhibition of AMPK by CC, although significantly reduced, could not abolish WSF-CT-11-induced glucose uptake (Figure 6B). This suggests that WSF-CT-11-induced Akt activation (upstream of AMPK) might also play roles in WSF-CT-11-induced glucose uptake by the inhibition of TBC1D4 and the promotion of GLUT4 translocation. In conclusion, AMPK and Akt and the downstream TBC1D1 and TBC1D4 might act synergistically on WSF-CT-11-induced GLUT4 translocation.³⁰

3.3. WSF-CT-11 Is a Potential Drug for Anti-diabetic Treatment. WSF-CT-11 might protect against T2D as a TRPV1 and AMPK activator. Evo, a widely used TRPV1 agonist, is a potential drug against T2D and related diseases. It is the active ingredient of *Evodia fructus*, a herbal drug against hypertension and stroke.³¹ In obese/diabetic mice, Evo could inhibit insulin-induced activation of mammalian target of rapamycin and ribosomal S6 protein kinase (S6K) (possibly by AMPK activation), suppress the negative feedback from S6K to IRS1, and thus increase insulin sensitivity.³²

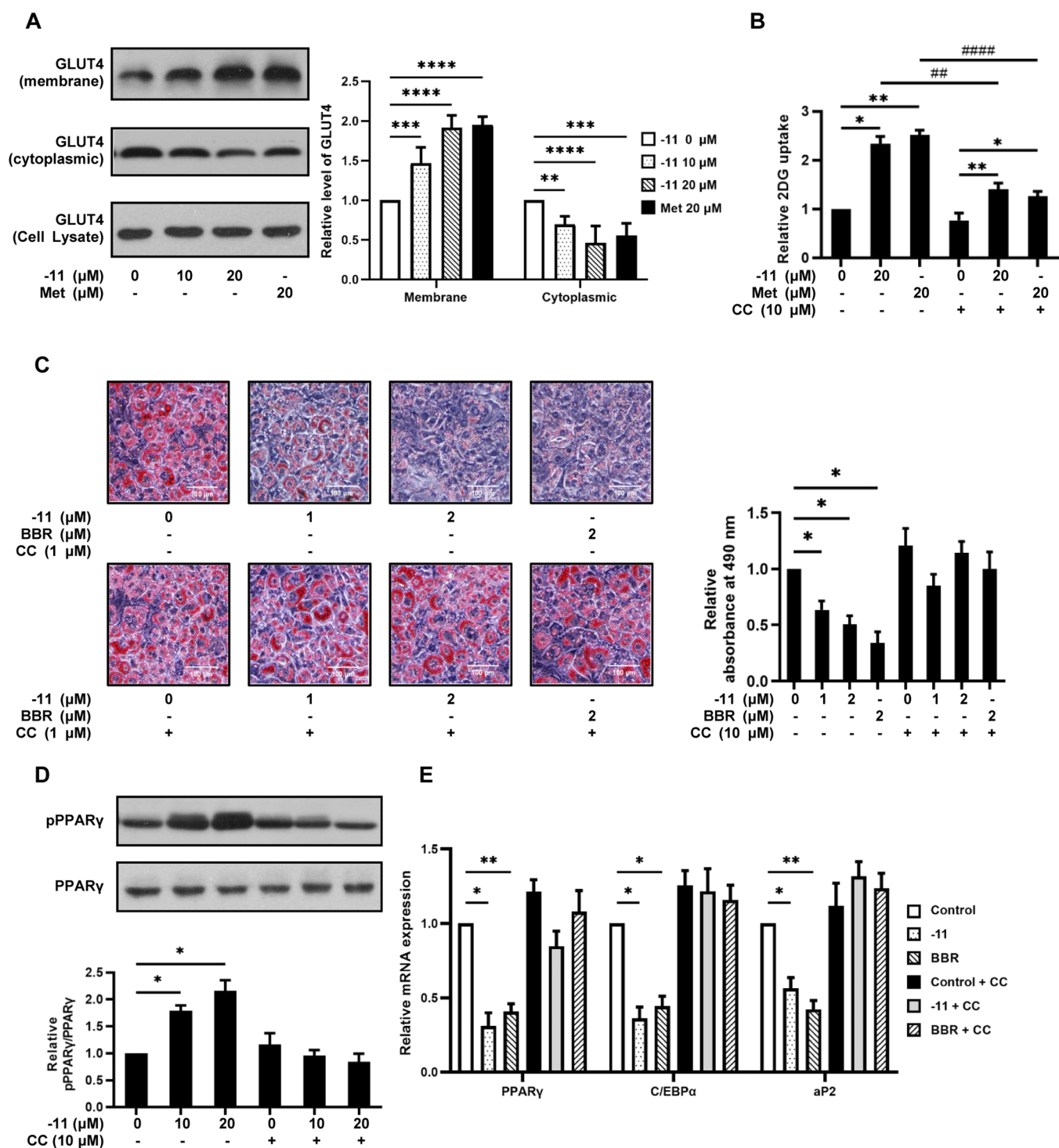


Figure 6. WSF-CT-11-induced AMPK activation could increase glucose uptake and inhibit adipogenesis in 3T3-L1 adipocytes. (A) 3T3-L1 adipocytes were treated with WSF-CT-11 (–11) or Met for 1 h and then subjected to membrane protein extraction. Levels of membrane proteins, cytoplasmic proteins, and total GLUT4 were determined by western blot. (B) 3T3-L1 adipocytes were treated with CC for 1 h and –11 or Met for another hour and then subjected to the glucose uptake assay. (C) 3T3-L1 preadipocytes were treated with –11 or BBR in the presence or absence of CC during differentiation and then stained with oil red. (D) 3T3-L1 adipocytes were treated with CC for 1 h and –11 for another hour and then immunoblotted for the levels of phospho-PPAR γ (Ser112) and PPAR γ . (E) Total RNA was isolated from 3T3-L1 adipocytes and subjected to qRT-PCR using primers for PPAR γ , C/EBP α , aP2, and β -actin. $n = 3$; * $p < 0.05$, ** $p < 0.01$, *** $p < 0.001$, **** $p < 0.0001$ vs vehicle-treated group; ## $p < 0.01$, ### $p < 0.0001$ vs Met-treated group.

WSF-CT-11 is a potential anti-diabetic drug as a synthetic derivative of sesquiterpene. The natural derivatives of sesquiterpene are widely reported to have anti-diabetic effects. For example, farnesene, a sesquiterpene hydrocarbon from

lemon balm, reduces hepatic gluconeogenesis and promotes adipose GLUT4 expression in *db/db* mice.³³ Atractylenolides, a sesquiterpene isolated from Baizhu, promote GLUT4 translocation and glucose uptake by the activation of PI3K/

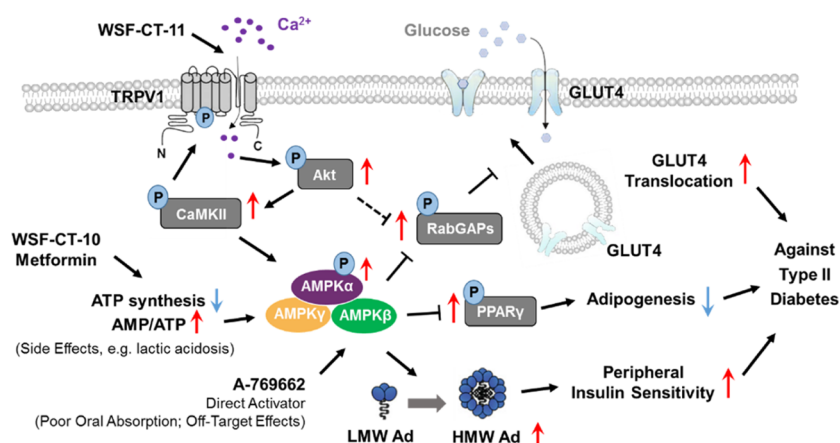


Figure 7. Schematic summary of this study. Unlike other activators that are associated with some side effects, -11 activates AMPK by activating TRPV1 and downstream Ca^{2+} -dependent PI3K/Akt/CaMKII signaling. -11-induced AMPK activation could promote GLUT4 translocation and glucose uptake, inhibit PPAR γ activity and adipogenesis, and improve the assembly of HMW Ad, thus increasing peripheral insulin sensitivity. Therefore, -11 is a potential drug against T2D and its comorbidities.

Akt signaling and AMPK in C2C12 myotubes.³⁴ β -Caryophyllene, a natural sesquiterpene lactone, could increase insulin secretion, restore antioxidant status, and thus ameliorate hyperglycemia in streptozotocin-induced diabetic rats.³⁵ In this study, we found that WSF-CT-11 could promote Ad assembly, increase glucose uptake, and inhibit adipogenesis in 3T3-L1 adipocytes. Therefore, it might be a potential drug against T2D and its comorbidities.

4. EXPERIMENTAL SECTION

4.1. Materials. Sesquiterpene derivatives were synthesized as described previously³⁶ and provided by Prof. Shifa Wang from the College of Chemical Engineering, Nanjing Forestry University. Other chemicals, for example, Met, Evo, BBR, EGTA, CC, CPZ, KN62, LY294002, protein A/G Sepharose, and nonspecific mouse IgG, were from Sigma-Aldrich (St. Louis, MO, USA). Rabbit antibodies for phospho-AMPK α (Thr172), phospho-CaMKII (Thr286), Akt, CaMKII, AMPK α , and GLUT4 and mouse antibodies against phospho-Akt (Ser473) and β -actin were from Cell Signaling (Beverly, MA, USA). Rabbit antibodies for phospho-PPAR γ (Ser112) and PPAR γ , mouse antibodies for phospho-TRPV1 (Ser502) and TRPV1, and Lipofectamine 3000 were from Invitrogen (Carlsbad, CA, USA). Small-interfering RNA (siRNA) targeting mouse AMPK α 1 (ACAUAUGCUGCAGGUGGA) and its scrambled control (UUAGGGCUGGAAUACGCA) were from GenePharma (Shanghai, China). Rabbit antibodies for the Ad monomer and multimers were prepared by an established method.¹³

4.2. Cell Culture. HEK293T cells and 3T3-L1 preadipocytes were obtained from ATCC and cultured in Dulbecco's modified Eagle's medium with 10% fetal bovine serum, 100 units/L penicillin, and 100 $\mu\text{g}/\text{mL}$ streptomycin at 37 $^{\circ}\text{C}$ in a 5% CO_2 incubator. Cells reach around 80% confluence before further treatment and are routinely tested for mycoplasma contamination.

To determine the anti-diabetic effects of WSF-CT-11-induced AMPK activation, 3T3-L1 preadipocytes were induced to differentiate by an established method.³⁷ For AMPK knockdown, 3T3-L1 adipocytes were transfected with AMPK α 1 siRNA (20 nmol/L) or scramble siRNA as a negative control by lipofectamine 3000 following the

manufacturer's instruction. The medium containing the transfection mix was replaced 24 h after transfection. Cells were then treated by WSF-CT-11 for another 24 h before western blot analysis. To explore whether WSF-CT-11-induced AMPK activation could promote GLUT4 translocation and glucose uptake in 3T3-L1 adipocytes, membrane proteins were isolated using the Mem-PER plus membrane protein extraction kit (Thermo Scientific, Waltham, MA USA). Glucose uptake assays were performed by Glucose Uptake-Glo assay kit (Promega, San Luis Obispo, CA, USA). The effect of WSF-CT-11-induced AMPK activation on adipogenesis was investigated by oil red Staining as previously described.³⁷

4.3. IP and Western Blot. HEK293T cells were cultured in 150 mm cell culture dishes to reach around 80% confluence and pretreated with inhibitors for 1 h and WSF-CT-11 for another hour. Cells were then lysed in Pierce IP lysis buffer with protease and phosphatase inhibitor cocktails (Thermo Scientific, Waltham, MA USA) and incubated with the antibody against TRPV1 or non-specific mouse IgG as a negative control overnight, followed by the incubation of protein A/G Sepharose for 2 h. Immune complexes were collected by centrifugation, washed with cold phosphate-buffered saline, and eluted in sodium dodecyl sulfate (SDS) lysis buffer (0.1% SDS, 0.5% sodium deoxycholate, 0.2% sodium azide, 1% Triton) with protease and phosphatase inhibitor cocktails.

For western blot, protein levels of cell lysates were measured by the bicinchoninic acid protein assay kit (Thermo Scientific, Waltham, MA, USA). Eluted samples were separated on SDS- or native-PAGE, transferred to poly(vinylidene difluoride) membranes, and then immunoblotted with primary and secondary antibodies. Bands were revealed by ECL detection kits (PerkinElmer, Waltham, MA, USA) and quantified by ImageJ (NIH, Bethesda, MD, USA).

4.4. Determination of Adenosine Phosphates and Ca^{2+} Levels in HEK293T Cells. For the measurement of AMP, adenosine 5'-diphosphate (ADP), and ATP levels, HEK293T cells were cultured in 100 mm cell culture dishes to reach 80% confluence, treated with WSF-CT-10, WSF-CT-11, or Met as a positive control for 1 h, then trypsinized, and collected. For the acid extraction of adenosine phosphates, 490 μL of 5% perchloric acid was added into the centrifugal tube, and the cells were disrupted by ultrasonic for 5 min in an ice

bath and neutralized with 80 μ L of 2 mol/L KOH solution. Then, the solution was centrifuged, and the levels of adenosine phosphates were measured in the supernatant by analytical HPLC, 1260 Infinity II LC System (Agilent Technologies, Santa Clara, CA, USA). The absorbance at 254 nm was detected. ATP, ADP, and AMP in the samples were identified according to the retention time of standards. The relative AMP/ATP ratio was determined by calculating the AMP/ATP peak area ratio and normalizing it against the control (vehicle-treated group).

For the determination of intracellular Ca^{2+} levels, HEK293T cells were cultured in 6-well plates to reach 80% confluence. Cells were treated with WSF-CT-10, WSF-CT-11, or Evo as a positive control for 1 h or pretreated with CPZ for 1 h, followed by the treatment of WSF-CT-11 or Evo for another hour. Cells were trypsinized, collected, and stained with Fluo-3 calcium indicator (Thermo Scientific, Waltham, MA, USA) for 1 h at room temperature. The intracellular Ca^{2+} concentration was then measured in the FL-1 channel on a BD LSRFortessa flow cytometer (BD, Pasadena, CA, USA). The relative Ca^{2+} levels were determined by collecting the mean fluorescent intensity and normalizing it against the control.

4.5. Reverse Transcription and qRT-PCR. 3T3-L1 preadipocytes were treated with WSF-CT-11 or BBR as a positive control during differentiation. Total RNA was extracted from the mature cells by an RNeasy Mini kit (QIAGEN, Hilden, Germany). The isolated RNA was quantified by a Qubit 4 fluorometer, and 1 mg of RNA was used for reverse transcription by a RevertAid First Strand cDNA synthesis kit (Thermo Scientific, Waltham, MA USA). qRT-PCR was performed by the QuantStudio 1 real-time PCR system (Applied Biosystems, South San Francisco, CA, USA). Expression data were normalized against the housekeeping gene β -actin. Primers used are listed as follows.

PPAR γ -forward: 5'-CTGGAATTAGATGACAGTGACTT-3'.

PPAR γ -reverse: 5'-CTCATGTCTGTCTCTGTCTTCT-3'.

C/EBP α -forward: 5'-TGCACCACCAACTGCTTAG-3'.

C/EBP α -reverse: 5'-AAACCATCCTCTGGGTCTCC-3'.

aP2-forward: 5'-ACATGATCATCAGCGTAAATGGG-3'.

aP2-reverse: 5'-TCATAACACATTCCACCACCAGC-3'.

β -Actin-forward: 5'-CACCAGGGTGTGATGGTGGGAAT-3'.

β -Actin-reverse: 5'-GGTCTTTACGGATGTCAACGTCA-CA-3'.

4.6. Statistical Analysis. Statistical analyses were performed by GraphPad Prism 9. Results are presented as mean \pm SD. Statistical significance was determined by one-way analysis of variance (ANOVA) with Dunnett's test or two-way ANOVA with Šidák's test as recommended. Statistical significance was denoted as * p < 0.05, ** p < 0.01, *** p < 0.001, **** p < 0.0001 versus vehicle-treated group and ## p < 0.01, #### p < 0.0001 versus Met-treated group. The experiments were replicated three times, and the representatives of at least three independent experiments are shown in the figures.

AUTHOR INFORMATION

Corresponding Authors

Shifa Wang – College of Chemical Engineering, Nanjing Forestry University, Jiangsu 210037, China; orcid.org/0000-0001-8578-9845; Phone: +86-138-1398-6152; Email: wangshifa65@163.com

Zhen Li – MOE Key Laboratory of Bioinformatics, School of Life Sciences, Tsinghua University, Beijing 100084, China; Phone: +86-135-5255-2601; Email: lizhen0581@hotmail.com, lizhen@mail.tsinghua.edu.cn

Authors

Yang Yang – MOE Key Laboratory of Bioinformatics, School of Life Sciences, Tsinghua University, Beijing 100084, China; orcid.org/0000-0001-6728-1159

Yunyun Wang – College of Chemical Engineering, Nanjing Forestry University, Jiangsu 210037, China

Zhijie Zhang – Institute of Chinese Materia Medica, China Academy of Chinese Medical Sciences, Beijing 100700, China

Complete contact information is available at:

<https://pubs.acs.org/10.1021/acsomega.1c05061>

Notes

The authors declare no competing financial interest.

ACKNOWLEDGMENTS

This work was supported by NSFC (nos. 31570760 and 31470592).

REFERENCES

- (1) Saeedi, P.; Petersohn, I.; Salpea, P.; Malanda, B.; Karuranga, S.; Unwin, N.; Colagiuri, S.; Guariguata, L.; Motala, A. A.; Ogurtsova, K.; Shaw, J. E.; Bright, D.; Williams, R. Global and regional diabetes prevalence estimates for 2019 and projections for 2030 and 2045: Results from the International Diabetes Federation Diabetes Atlas, 9th edition. *Diabetes Res. Clin. Pract.* **2019**, *157*, 107843.
- (2) Chobot, A.; Gorowska-Kowolik, K.; Sokolowska, M.; Jarosz-Chobot, P. Obesity and diabetes-Not only a simple link between two epidemics. *Diabetes/Metab. Res. Rev.* **2018**, *34*, No. e3042.
- (3) Lee, J. O.; Lee, S. K.; Kim, J. H.; Kim, N.; You, G. Y.; Moon, J. W.; Kim, S. J.; Park, S. H.; Kim, H. S. Metformin regulates glucose transporter 4 (GLUT4) translocation through AMP-activated protein kinase (AMPK)-mediated Cbl/CAP signaling in 3T3-L1 preadipocyte cells. *J. Biol. Chem.* **2012**, *287*, 44121–44129.
- (4) Coughlan, K. A.; Valentine, R. J.; Ruderman, N. B.; Saha, A. K. AMPK activation: a therapeutic target for type 2 diabetes? *Diabetes, Metab. Syndr. Obes.: Targets Ther.* **2014**, *7*, 241–253.
- (5) Hardie, D. G.; Ross, F. A.; Hawley, S. A. AMPK: a nutrient and energy sensor that maintains energy homeostasis. *Nat. Rev. Mol. Cell Biol.* **2012**, *13*, 251–262.
- (6) Hawley, S. A.; Ross, F. A.; Chevtzoff, C.; Green, K. A.; Evans, A.; Fogarty, S.; Towler, M. C.; Brown, L. J.; Ogunbayo, O. A.; Evans, A. M.; Hardie, D. G. Use of cells expressing gamma subunit variants to identify diverse mechanisms of AMPK activation. *Cell Metab.* **2010**, *11*, 554–565.
- (7) Ching, L.-C.; Chen, C.-Y.; Su, K.-H.; Hou, H.-H.; Shyue, S.-K.; Kou, Y. R.; Lee, T.-S. Implication of AMP-activated protein kinase in transient receptor potential vanilloid type 1-mediated activation of endothelial nitric oxide synthase. *Mol. Med.* **2012**, *18*, 805–815.
- (8) Esteve Ràfols, M. Adipose tissue: Cell heterogeneity and functional diversity. *Endocrinol. Nutr.* **2014**, *61*, 100–112.
- (9) Fang, H.; Judd, R. L. Adiponectin Regulation and Function. *Compr. Physiol.* **2018**, *8*, 1031–1063.
- (10) Lihn, A. S.; Pedersen, S. B.; Richelsen, B. Adiponectin: action, regulation and association to insulin sensitivity. *Obes. Rev.* **2005**, *6*, 13–21.
- (11) Waki, H.; Yamauchi, T.; Kamon, J.; Ito, Y.; Uchida, S.; Kita, S.; Hara, K.; Hada, Y.; Vasseur, F.; Froguel, P.; Kimura, S.; Nagai, R.; Kadowaki, T. Impaired multimerization of human adiponectin mutants associated with diabetes. Molecular structure and multimer formation of adiponectin. *J. Biol. Chem.* **2003**, *278*, 40352–40363.

- (12) Briggs, D. B.; Jones, C. M.; Mashalidis, E. H.; Nuñez, M.; Hausrath, A. C.; Wysocki, V. H.; Tsao, T.-S. Disulfide-Dependent Self-Assembly of Adiponectin Octadecamers from Trimers and Presence of Stable Octadecameric Adiponectin Lacking Disulfide Bonds *in Vitro*. *Biochemistry* **2009**, *48*, 12345–12357.
- (13) Pajvani, U. B.; Hawkins, M.; Combs, T. P.; Rajala, M. W.; Doebber, T.; Berger, J. P.; Wagner, J. A.; Wu, M.; Knopps, A.; Xiang, A. H.; Utzschneider, K. M.; Kahn, S. E.; Olefsky, J. M.; Buchanan, T. A.; Scherer, P. E. Complex distribution, not absolute amount of adiponectin, correlates with thiazolidinedione-mediated improvement in insulin sensitivity. *J. Biol. Chem.* **2004**, *279*, 12152–12162.
- (14) Klip, A.; McGraw, T. E.; James, D. E. Thirty sweet years of GLUT4. *J. Biol. Chem.* **2019**, *294*, 11369–11381.
- (15) Bryant, N. J.; Gould, G. W. Insulin stimulated GLUT4 translocation - Size is not everything. *Curr. Opin. Cell Biol.* **2020**, *65*, 28–34.
- (16) Lee, Y. S.; Kim, W. S.; Kim, K. H.; Yoon, M. J.; Cho, H. J.; Shen, Y.; Ye, J.-M.; Lee, C. H.; Oh, W. K.; Kim, C. T.; Hohnen-Behrens, C.; Gosby, A.; Kraegen, E. W.; James, D. E.; Kim, J. B. Berberine, a natural plant product, activates AMP-activated protein kinase with beneficial metabolic effects in diabetic and insulin-resistant states. *Diabetes* **2006**, *55*, 2256–2264.
- (17) Ching, L.-C.; Kou, Y. R.; Shyue, S.-K.; Su, K.-H.; Wei, J.; Cheng, L.-C.; Yu, Y.-B.; Pan, C.-C.; Lee, T.-S. Molecular mechanisms of activation of endothelial nitric oxide synthase mediated by transient receptor potential vanilloid type 1. *Cardiovasc. Res.* **2011**, *91*, 492–501.
- (18) Liu, L.-H.; Xie, J.-Y.; Guo, W.-W.; Wu, G.-Y.; Chen, Z.-F.; Yi, J.-Y.; Zhang, L.; Zhang, Z.-J.; Li, Z. Evodiamine activates AMPK and promotes adiponectin multimerization in 3T3-L1 adipocytes. *J. Asian Nat. Prod. Res.* **2014**, *16*, 1074–1083.
- (19) Maeda, N.; Takahashi, M.; Funahashi, T.; Kihara, S.; Nishizawa, H.; Kishida, K.; Nagaretani, H.; Matsuda, M.; Komuro, R.; Ouchi, N.; Kuriyama, H.; Hotta, K.; Nakamura, T.; Shimomura, L.; Matsuzawa, Y. PPAR gamma ligands increase expression and plasma concentrations of adiponectin, an adipose-derived protein. *Diabetes* **2001**, *50*, 2094–2099.
- (20) Lee, J.-E.; Ge, K. Transcriptional and epigenetic regulation of PPAR γ expression during adipogenesis. *Cell Biosci.* **2014**, *4*, 29–39.
- (21) Burns, K.; Vandenheuveel, J. Modulation of PPAR activity via phosphorylation. *Biochim. Biophys. Acta* **2007**, *1771*, 952–960.
- (22) Leff, T. AMP-activated protein kinase regulates gene expression by direct phosphorylation of nuclear proteins. *Biochem. Soc. Trans.* **2003**, *31*, 224–227.
- (23) Christie, S.; Wittert, G. A.; Li, H.; Page, A. J. Involvement of TRPV1 Channels in Energy Homeostasis. *Front. Endocrinol.* **2018**, *9*, 420–433.
- (24) Iftinca, M.; Defaye, M.; Altier, C. TRPV1-Targeted Drugs in Development for Human Pain Conditions. *Drugs* **2021**, *81*, 7–27.
- (25) Yang, D.; Luo, Z.; Ma, S.; Wong, W. T.; Ma, L.; Zhong, J.; He, H.; Zhao, Z.; Cao, T.; Yan, Z.; Liu, D.; Arendshorst, W. J.; Huang, Y.; Tepel, M.; Zhu, Z. Activation of TRPV1 by dietary capsaicin improves endothelium-dependent vasorelaxation and prevents hypertension. *Cell Metab.* **2010**, *12*, 130–141.
- (26) Schnizler, K.; Shutov, L. P.; Van Kanegan, M. J.; Merrill, M. A.; Nichols, B.; McKnight, G. S.; Strack, S.; Hell, J. W.; Usachev, Y. M. Protein kinase A anchoring via AKAP150 is essential for TRPV1 modulation by forskolin and prostaglandin E2 in mouse sensory neurons. *J. Neurosci.* **2008**, *28*, 4904–4917.
- (27) Richter, E. A.; Hargreaves, M. Exercise, GLUT4, and skeletal muscle glucose uptake. *Physiol. Rev.* **2013**, *93*, 993–1017.
- (28) Foley, K.; Boguslavsky, S.; Klip, A. Endocytosis, Recycling, and Regulated Exocytosis of Glucose Transporter 4. *Biochemistry* **2011**, *50*, 3048–3061.
- (29) Taylor, E. B.; An, D.; Kramer, H. F.; Yu, H.; Fujii, N. L.; Roeckl, K. S. C.; Bowles, N.; Hirshman, M. F.; Xie, J.; Feener, E. P.; Goodyear, L. J. Discovery of TBC1D1 as an insulin-, AICAR-, and contraction-stimulated signaling nexus in mouse skeletal muscle. *J. Biol. Chem.* **2008**, *283*, 9787–9796.
- (30) Hatakeyama, H.; Morino, T.; Ishii, T.; Kanzaki, M. Cooperative actions of Tbc1d1 and AS160/Tbc1d4 in GLUT4-trafficking activities. *J. Biol. Chem.* **2019**, *294*, 1161–1172.
- (31) Xu, S. B.; Huang, Y. M.; Lau, C. N. B.; Wat, C. K. H.; Kong, Y. C. Hypotensive Effect of Dehydroevodiamine from *Evodiae Fructus*. *Am. J. Chin. Med.* **1982**, *10*, 75–85.
- (32) Wang, T.; Kusudo, T.; Takeuchi, T.; Yamashita, Y.; Kontani, Y.; Okamatsu, Y.; Saito, M.; Mori, N.; Yamashita, H. Evodiamine inhibits insulin-stimulated mTOR-S6K activation and IRS1 serine phosphorylation in adipocytes and improves glucose tolerance in obese/diabetic mice. *PLoS One* **2013**, *8*, No. e83264.
- (33) Chung, M. J.; Cho, S.-Y.; Bhuiyan, M. J. H.; Kim, K. H.; Lee, S.-J. Anti-diabetic effects of lemon balm (*Melissa officinalis*) essential oil on glucose- and lipid-regulating enzymes in type 2 diabetic mice. *Br. J. Nutr.* **2010**, *104*, 180–188.
- (34) Chao, C.-L.; Huang, H.-C.; Lin, H.-C.; Chang, T.-C.; Chang, W.-L. Sesquiterpenes from Baizhu Stimulate Glucose Uptake by Activating AMPK and PI3K. *Am. J. Chin. Med.* **2016**, *44*, 963–979.
- (35) Basha, R. H.; Sankaranarayanan, C. beta-Caryophyllene, a natural sesquiterpene lactone attenuates hyperglycemia mediated oxidative and inflammatory stress in experimental diabetic rats. *Chem. Biol. Interact.* **2016**, *245*, 50–58.
- (36) Wang, Y.; Wu, C.; Zhang, Q.; Shan, Y.; Gu, W.; Wang, S. Design, synthesis and biological evaluation of novel beta-pinene-based thiazole derivatives as potential anticancer agents via mitochondrial-mediated apoptosis pathway. *Bioorg. Chem.* **2019**, *84*, 468–477.
- (37) Lee, H.; Kang, R.; Bae, S.; Yoon, Y. AICAR, an activator of AMPK, inhibits adipogenesis via the WNT/beta-catenin pathway in 3T3-L1 adipocytes. *Int. J. Mol. Med.* **2011**, *28*, 65–71.